Smart Structures and Systems, Vol. 1, No. 4 (2005) 339-353
DOI: http://dx.doi.org/10.12989/sss.2005.1.4.339

Health monitoring of steel structures using impedance of thickness modes at PZT patches

Seunghee Park† and Chung-Bang Yun‡

Department of Civil and Environmental Engineering, KAIST, Korea

Yongrae Roh‡†

School of Mechanical Engineering, Kyungpook National University, Korea

Jong-Jae Lee‡‡

Department of Civil and Environmental Engineering, KAIST, Korea

(Received August 20, 2004, Accepted October 10, 2005)

Abstract. This paper presents the results of a feasibility study on an impedance-based damage detection technique using thickness modes of piezoelectric (PZT) patches for steel structures. It is newly proposed to analyze the changes of the impedances of the thickness modes (frequency range > 1 MHz) at the PZT based on its resonant frequency shifts rather than those of the lateral modes (frequency range > 20 kHz) at the PZT based on its root mean square (RMS) deviations, since the former gives more significant variations in the resonant frequency shifts of the signals for identifying localities of small damages under the same measurement condition. In this paper, firstly, a numerical analysis was performed to understand the basics of the NDE technique using the impedance using an idealized 1-D electro-mechanical model consisting of a steel plate and a PZT patch. Then, experimental studies were carried out on two kinds of structural members of steel. Comparisons have been made between the results of crack detections using the thickness and lateral modes of the PZT patches.

Keywords: structural health monitoring; PZT; electro-mechanical impedance; thickness modes; crack detection; steel structures.

1. Introduction

Recently, research and development activities on structural health monitoring (SHM) led to the development of smart sensors and IT-based smart sensing/monitoring systems in the fields of mechanical, aeronautical and civil engineering. SHM technology is essentially aimed at the development of autonomous systems for continuous monitoring and integrity assessment of structures with minimum labor involvement. Therefore, a smart wireless monitoring system and low-cost but high-effect smart sensors such as piezoelectric sensor,

†Ph.D. Candidate, Corresponding Author, E-mail: shparkpc@kaist.ac.kr
‡Professor, E-mail: ycb@kaist.ac.kr
‡†Professor, E-mail: yryong@knu.ac.kr
‡‡Post Doctoral Researcher, E-mail: jongjae@kaist.ac.kr

optical fiber sensor, and micro-electromechanical system (MEMS) sensor are needed to be developed. In particular, the impedance-based technique, which uses smart piezoelectric materials, has emerged as a powerful tool for SHM (Raju, *et al*. 1998, Park, *et al*. 2003, Zagrai and Giurgiutiu 2001). In this study, a PZT patch, as a kind of piezoelectric ceramic materials, is bonded to a structure and a high-fidelity electro-mechanical impedance signature of the patch serves as a diagnostic signature of the structure (Sun, *et al*. 1994, Giurgiutiu and Rogers 1997). Physical changes in the structure cause changes in the structural mechanical impedance, which may induce changes in the electrical impedance of the PZT patch. Those changes in the impedances of the PZT patches are used to identify incipient damages in the structure. The applications of the PZT to civil structures began relatively recently Ayres, *et al.* (1998) reported on the use of the PZT for damage detection on a laboratory sized truss structure and a prototype truss joint. Tseng, *et al.* (2000), Soh, *et al.* (2000), and Bhalla, *et al.* (2003) recently reported successful applications of this method on concrete and other civil-infrastructures. Park, *et al.* (2000) reported the successful use of the PZT on the damage detection for both a composite reinforced-concrete wall and a 1/4-scale steel bridge section. Even though many other previous researches (Raju, *et al*. 1998, Park, *et al*. 2003, Zagrai and Giurgiutiu 2001, Ayres, *et al.* 1998, Tseng, *et al.* 2000, Soh, *et al.* 2000, and Bhalla, *et al.* 2003) have considered the changes of a lateral mode-impedance (frequency range>20 kHz) at the PZT based on its root mean square (RMS) deviations, in this study, the concept to utilize the changes of a thickness mode-impedance (frequency range>1 MHz) at the PZT based on its resonant frequency shifts is newly proposed. By operating the thickness mode-vibrations at higher frequencies, this technique shows more significant variations in resonant frequency shifts of the signals for identifying localities of incipient and small damages.

In this paper, firstly, a numerical analysis was performed to understand the basics of the NDE technique using the impedance using an idealized 1-D electro-mechanical model consisting of a steel plate and a PZT patch. Then, experimental studies were carried out on two kinds of steel structural members for identification of damages such as cracks. Comparisons have been made between the results for crack detections using the thickness and lateral modes of the PZT patches. The results of the experimental studies showed the powerful applicability of the damage detection technique using the thickness mode-impedance of PZT patches for steel structures.

2. Basics of impedance-based NDE technique

2.1. Electro-mechanical impedance

The coupling effect of the electro-mechanical impedance of a system with a PZT patch and a host

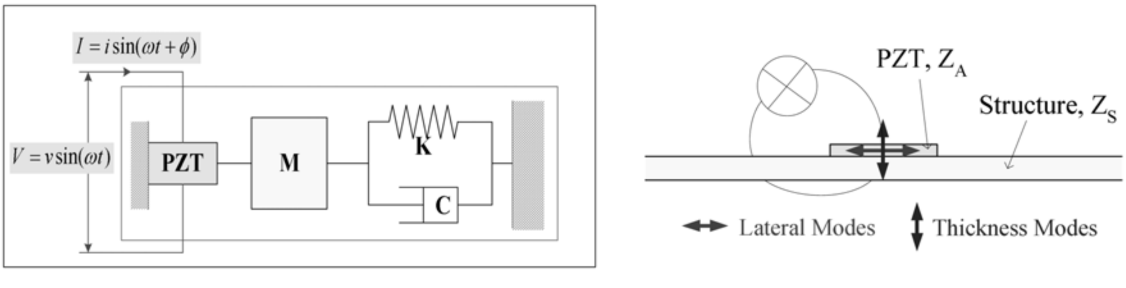

Fig. 1 1-D electro-mechanical impedance system (Giurgiutiu and Rogers 1997) structure can be conceptually investigated by using an idealized 1-D electro-mechanical system as shown in Fig. 1 (Giurgiutiu and Rogers 1997). The electrical aspect of the PZT is described by its short-circuited impedance, and the host structure is represented by its driving point mechanical impedance, which includes the effect of mass, stiffness, damping and boundary conditions.

The PZT is powered by voltage or current. The integrated electro-mechanical system may be electrically represented by an electrical impedance which is affected by the dynamics of the PZT and the host structure. The mechanical impedance, Z_A of the PZT patch as in Fig. 1 is defined as the ratio of a harmonic input voltage $V(\omega)$ at an angular frequency ω to the current response $I(\omega)$ in frequency domain. Similarly, the mechanical impedance, Z_S of the host structure idealized as a SDOF system, is defined as the ratio of a harmonic excitation force $F_0(\omega)$ at an angular frequency ω to the velocity response $\dot{x}(\omega)$ in frequency domain. At first, if the lateral vibration mode of the PZT patch is taken into account, the apparent electro-mechanical impedance of the PZT as coupled to the host structure is obtained as Eq. (1).

$$Z_{total}(\omega) = \left\{ j\omega \frac{wl}{s}\left[\frac{d_{31}^2 Y_{11}^E Z_A(\omega)}{Z_A(\omega)+Z_S(\omega)}\frac{\tan(\kappa l)}{\kappa l} + \varepsilon_{33}^T - d_{31}^2 Y_{11}^E\right]\right\}^{-1} \tag{1}$$

where Z_A is the impedance of the PZT patch, and Z_S is the loading impedance of the host structure obtained as

$$Z_A(\omega) = \frac{V(\omega)}{I(\omega)} = \frac{\kappa w s Y_{xx}^E}{(j\omega)\tan(\kappa l)} \tag{2}$$

$$Z_S(\omega) = \frac{F_0(\omega)}{\dot{x}_0(\omega)} = c + j\left(\frac{m\omega^2 - k}{\omega}\right) \tag{3}$$

in which κ is a wave number ($=\omega/c_t^E$); ω is an excitation frequency; c_t^E is a wave velocity ($=\sqrt{Y_{xx}^E/\rho}$); ρ is density; Y_{xx}^E is an elastic stiffness at a constant electric field; d_{3x} is the piezoelectric strain coefficient; ε_{33}^T is a permittivity at constant stress; l is a PZT length; w is a PZT width; s is a PZT thickness; F_0 is a resultant force; $\dot{x}_0$ is the amplitude of an instantaneous velocity response; and m, c and k are mass, damping and stiffness of the host structure.

Most reported studies on the PZT impedance-based non-destructive evaluations (NDE) (Raju, *et al.* 1998, Park, *et al.* 2003, Zagrai and Giurgiutiu 2001, Ayres, *et al.* 1998, Tseng, *et al.* 2000, Soh, *et al.* 2000, and Bhalla, *et al.* 2003) utilized the impedance signatures in the lateral modes as described in above equations. In this study, however, the impedance of the PZT patch in the thickness modes is mainly utilized. For the thickness mode-impedance, the patch dimensions correspondent to vibration mode direction in Eqs. (1) and (2) will be simply exchanged each other (i.e. l for lateral modes and s for thickness modes). And also, the material properties of the PZT patch which depend on the vibration mode direction should be changed into corresponding values. (i.e. Y_{11}^E and d_{31} for lateral modes into Y_{33}^E and d_{33} for thickness modes) That is, their coupling factors must be different from each other.

The electro-mechanical impedance technique permits damage detections, health monitoring, and *built-in* NDE because it can measure directly the high frequency local impedance which is very sensitive to local damage. This method utilizes the changes that take place in the high-frequency drive-point structural impedance to identify incipient damage in the structure. Hence, changes of the mechanical properties of the host structure may be detected by monitoring the variations of the electro-mechanical impedance functions shown in Eq. (1). In this study, particularly, the PZT patches in which the thickness is much smaller than the length are used. Therefore, the fundamental resonant frequency for the thickness vibration modes is generally larger than 1 MHz, while that for the lateral vibration modes is in the order of 20 kHz. According to Sauerbrey Equation (Sauerbrey 1959) which indicates that the frequency shifts in the dominant peaks of the impedance signature of the PZT patch are proportional to the square of its fundamental resonant frequency, it is expected that some changes of the mechanical properties of the host structure may cause much more significant variations in the resonant frequency shifts of the electro-mechanical impedance functions of the PZT patch in the thickness modes rather than in the lateral modes.

2.2. Numerical study for impedance-based NDE

A numerical study was carried out for an imaginary thin plate structure to investigate the applicability of the impedance-based NDE technique using the PZT patch. The thin plate structure and a typical PZT patch are modeled using an 1-D interaction model as shown in Fig. 2. Eventually, the damages in the host structures may affect its characteristic impedance (Z_C) and the acoustic wave velocity (c_t^E) of the PZT impedance. Therefore, in this analysis, structural damages can be simulated by the variations of the characteristic impedance in the host structure and the wave number (κ) of the PZT impedance. Herein, the characteristic impedance of the host structure can be defined as in Eq. (4) (Kinsler and Frey 1962).

$$Z_C = \rho \cdot c = \sqrt{\rho \cdot E} \tag{4}$$

where ρ is a material density, c is a sound velocity, and E is Young's modulus.

The dimension of the PZT patch is assumed as 12×12×0.5 (mm). Details of the assumed material properties of the model are described as in Table 1 (2005). Through the substitution of these values for corresponding parameters in Eqs. (1), (2) and (4), the electro-mechanical impedance signatures have been calculated. The variations of the impedance signatures caused by the reduction of the characteristic impedance (ΔZ_C) of the host structure and the increase of the wave number ($\Delta\kappa$) of the PZT impedance have been investigated in Fig. 3. Herein, it can be found that the impedance signatures for the thickness modes exhibit more appreciable sensitivity in the resonant frequencies and their peak values due to the presence of damages than those for the lateral modes. The results verified that damages in the host structure may be more efficiently detected by monitoring the changes in the

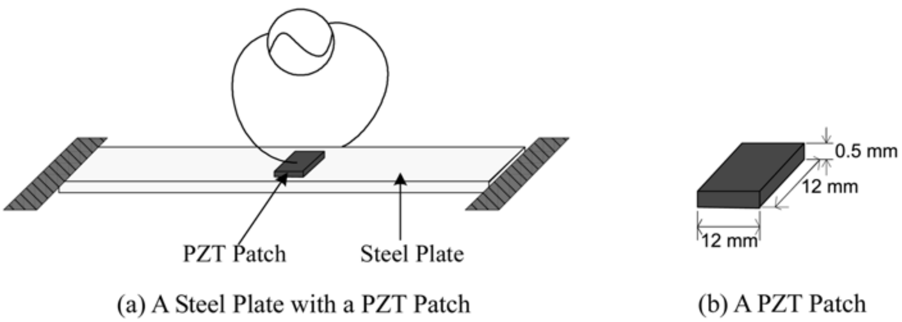

Fig. 2 Models for numerical analysis

Table 1 Material properties (Morgan Electro Ceramics (2005))

PZT patch (PZT 5H)	
Density, ρ (kg/m^3)	7450
Electric Stiffness, Y_{11}^E / Y_{33}^E (N/m^2)	$6.2\times10^{10}/4.8\times10^{10}$
Piezoelectric Strain Constant, d_{31}/d_{33}(C/V)	$-2.74\times10^{-10}/5.93\times10^{-10}$
Elastic Permittivity, ε_{33}^D (F/m)	3.01×10^{-8}
Steel plate	
Density, ρ (kg/m^3)	7850
Young's modulus, E (N/m^2)	2×10^{11}

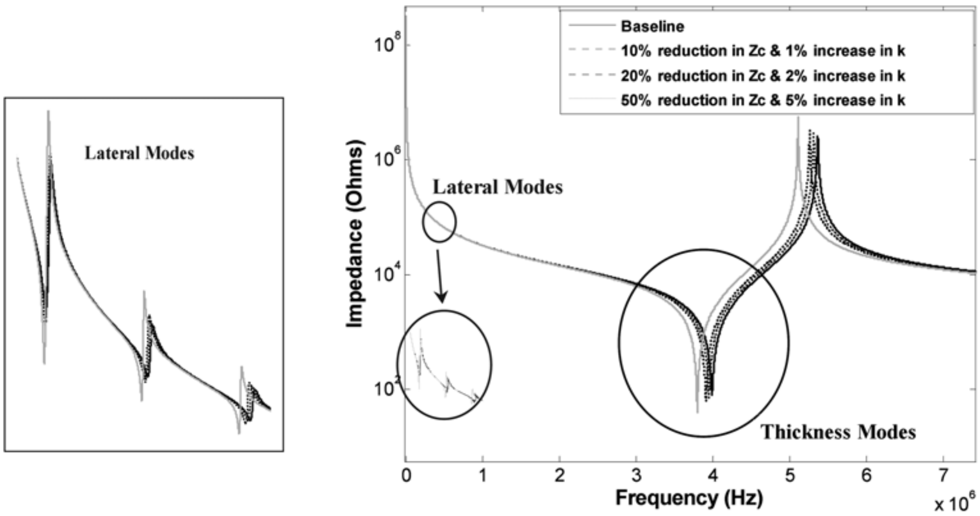

Fig. 3 Impedance signatures at PZT patch through numerical study

electro-mechanical impedance of the thickness modes at the PZT attached to the structure. Note that this analysis did not account for the model which simulates real damages of the host structure. The development of a more complicated model for real damages is currently pursued to capture the dynamics of this analysis in a more quantitative manner.

3. Experimental studies

3.1. Experimental setup and procedures

The experimental setup consists of a test specimen, PZT patches, an impedance analyzer, and a personal computer (PC) equipped with data acquisition software as shown in Fig. 4. PZT patches are bonded to the specimen, and they are connected to the HP4294A (impedance analyzer). Then, the impedance signatures are extracted as functions of the exciting frequency. The PC is used to control the impedance analyzer.

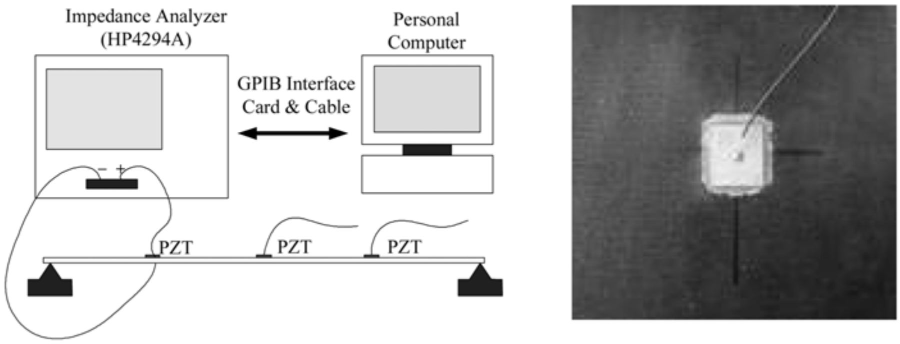

Fig. 4 Experimental setup and PZT patch

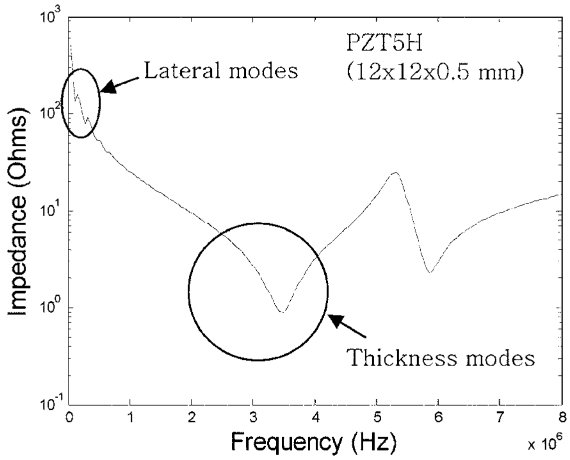

Fig. 5 Selection of frequency ranges from impedance signatures (PZT5H (12×12×0.5 mm) on Steel Plate)

3.2. Frequency range

In order to select a suitable frequency range for acquiring the impedance signature, the PZT patches on the test specimen are scanned over a wide frequency range of 20 kHz-8 MHz as shown in Fig. 5. The real signatures show many sharp peaks over a wide range of frequency. Two frequency ranges are chosen in order to compare the effect of different vibration modes on damage assessment: 30-500 kHz for lateral modes and 1-5 MHz for thickness modes. These signatures consist of a total of 400 data points, with some dominant peaks observed in these ranges. Actually, many other previous researchers have considered the frequency range of 30-500 kHz, which is selected for the lateral modes of the PZT. However, in this study, the range of 1-5 MHz pertaining to the thickness modes of the PZT is additionally chosen.

3.3. Damage index approach

The prominent effects of damage in the host structure on the impedance signature are the appearance of new peaks in the signature and the lateral and vertical shifts of the existing peaks. Traditionally, statistical pattern recognition techniques have been employed to quantify changes in the impedance signature due to damage; such as relative deviation (RD), root mean square (RMS) deviation, and mean absolute percentage (MPA) deviation. The RMS deviation index is used in this study as

$$RMSD(\%) = \sqrt{\frac{\sum_{i=1}^{i=N}(Z(\omega_i) - Z_0(\omega_i))^2}{\sum_{i=1}^{i=N}(Z_0(\omega_i))^2}} \times 100 \tag{5}$$

where $Z(\omega_i)$ is the post-damage impedance signature at the i-th measurement point and $Z_0(\omega_i)$ is the corresponding pre-damage value.

However, if the thickness mode-impedance at the PZT patches is considered, the resonant frequency shifts of the impedance signatures can be used as a simpler damage indicator.

$$\Delta\omega = \left|\omega_0^d - \omega_0\right| \tag{6}$$

where $\omega_0{}^d$ is the post-damage resonant frequency at the impedance signature and ω_0 is the pre-damage resonant frequency value.

In many structures, the damage detection might be more than sufficient, which can be done conveniently by means of conventional statistical indices. However, in the civil infrastructures, we often need to find out whether the damage is ‘incipient’ or ‘severe’. We might even tolerate an incipient damage without endangering lives or properties. This fact has motivated us to extract the structural impedance from the measured impedance signatures for damage quantification. Studies for calibrating the changes in the impedance signatures with damage for typical civil infrastructures will be studied in the future.

3.4. Results and discussion

3.4.1. Example I: steel plate with cracks

A thin steel strip was used as a test specimen as shown in Fig. 6. It is 100 cm long, 10 cm wide, and 0.6 cm thick. Three PZT patches of 10×10×0.5 mm are bonded to the specimen with the same distance. Two cracks with length of 2.5 cm and 3.0 cm were introduced near PZTs 1 and 2 (2 cm apart from each PZT patch) sequentially as in Fig. 6. Therefore, Damage Case I-1 has a crack near PZT 1, while Damage Case I-2 consists of two cracks near PZTs 1 and 2. Impedance signatures were assessed for both lateral modes and thickness modes at the PZT patches for the intact and two damage cases, and the results are shown in Figs. 7 and 8, respectively.

As mentioned above, it can be observed from Fig. 8 that the impedance functions change more significantly in magnitudes and resonant frequencies, as cracks occur near the sensors. The decrease of the resonant frequencies is summarized for two damage cases at Table 2. The amounts of the frequency shifts are found to be very noticeable at the PZTs near the cracks. For instance, in Damage

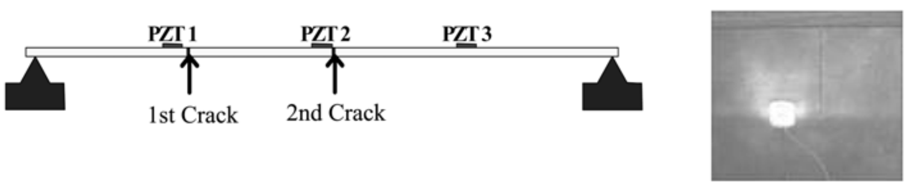

Fig. 6 Test specimen I

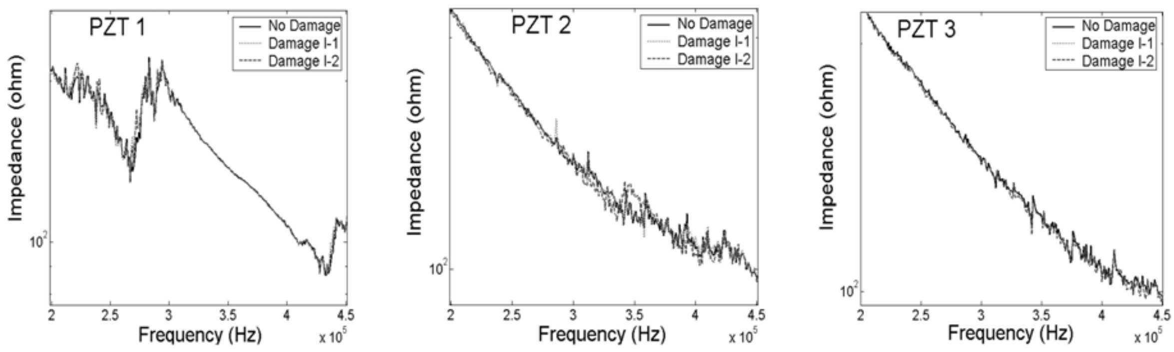

(a) PZT 1 (b) PZT 2 (3) PZT 3

Fig. 7 Impedance signatures of lateral modes at PZT patches (in Magnitudes)

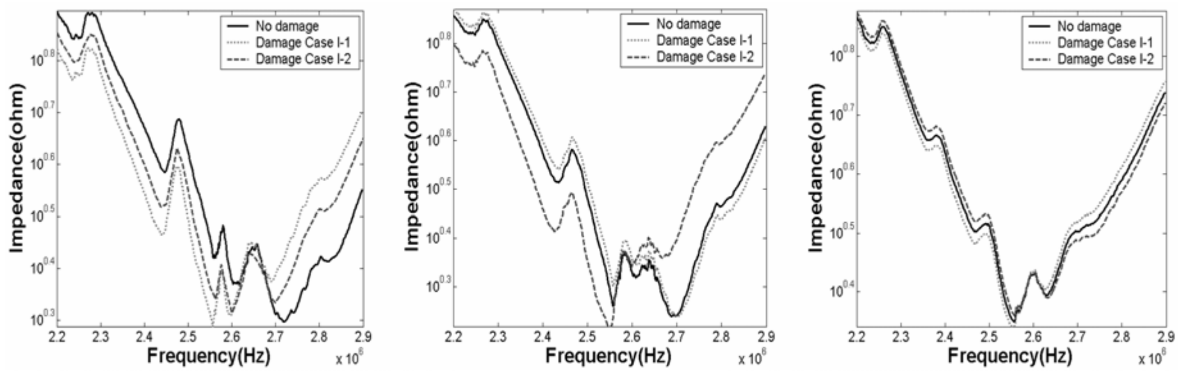

(a) PZT 1 (b) PZT 2 (3) PZT 3

Fig. 8 Impedance signatures of thickness modes at PZT patches (in Magnitudes)

Table 2 Resonant frequencies and frequency shifts of Example I (in Hz)
(Note: The values in the parentheses are the shifts of resonant frequencies from Intact Case)

Damage cases	PZT1	PZT2	PZT3
No damage	2719750 (0)	2697000 (0)	2557000 (0)
Damage Case I-1	2690000 (-29750)	2700500 (3500)	2555250 (-1750)
Damage Case I-2	2698750 (-21000)	2679500 (-17500)	2557000 (0)

Case I-1, the resonant frequency at PZT 1 reduces by 29.75 kHz due to a crack near PZT 1, while the shifts at PZTs 2 and 3 are only 1.75 and 3.5 kHz, respectively. The frequency resolution of HP4294A impedance analyzer was 1.75 kHz. In Damage Case I-2, the resonant frequency at PZT 2 shifts by 17.5 kHz due to an additional crack near PZT 2, while the corresponding shifts at PZTs 1and 3 are very minimal.

The RMS deviation was also considered for both lateral modes and thickness modes at PZTs as a damage indicator, and the results are shown in Figs. 9 and 10, respectively. They show the effects of damages (simulated by cutting 2.5 cm and 3.0 cm cracks) on the impedance signature of a PZT patch

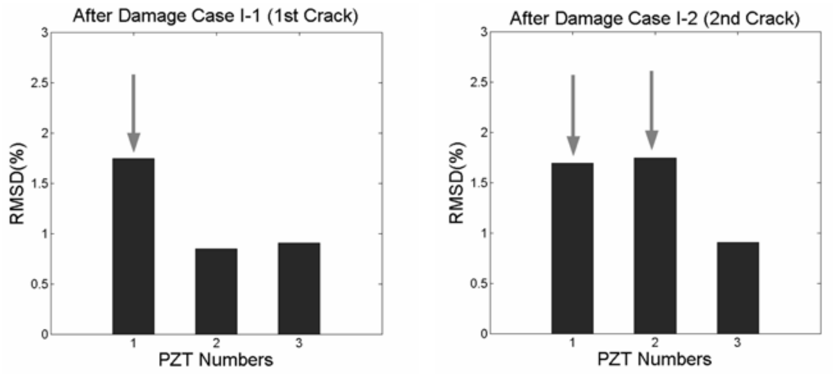

(a) Damage I-1 (b) Damage I-2

Fig. 9 RMS deviations of impedance functions of lateral modes at PZTs
(Note: Arrows indicate the locations of cracks.)

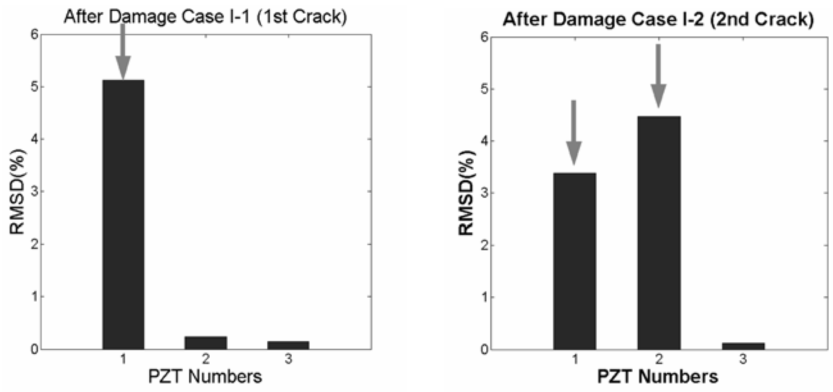

(a) Damage I-1 (b) Damage I-2

Fig. 10 RMS deviations of impedance functions of thickness modes at PZTs
(Note: Arrows indicate the locations of cracks.)

bonded to a steel plate. From the Figs. 9 and 10, it can be found that the RMS deviations for both lateral modes and thickness modes give us good information as damage indicators. Especially, Fig. 10 corresponding to the thickness modes shows the more significant damage localization results compared with the Fig. 9 related to the lateral modes. Therefore, it can be concluded that the method using the thickness modes of the PZTs gives the results which have better sensitivity and more significant shifts in the resonant frequencies than the lateral modes-based method for identifying the localities of small cracks.

3.4.2. Example II: steel member with welded zone of two flanges

The second example is a vertical steel member as shown in Fig. 11. It is a 1/8-scale model of a vertical truss member of old Seongsoo Bridge in Seoul Korea, which caused the collapse of a Gerber section in the middle of a span in 1994. The original member consists of two segments with wide flange sections of different flange thickness welded together as in Fig. 11(a). Fatigue cracks developed at the

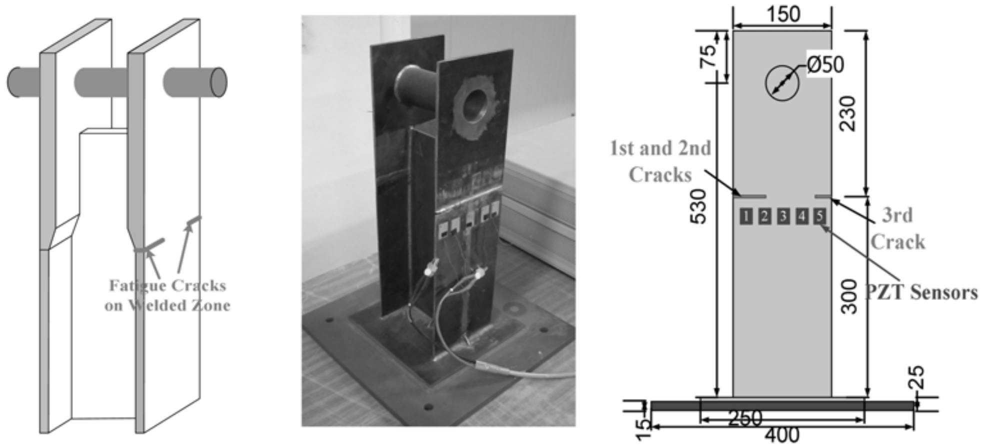

(a) Vertical Truss Member in Seongsoo Bridge (b) Test Specimen: 1/8-Scale Model (c) PZT Sensors and Cracks on a Flange (in mm)

Fig. 11 Test specimen II

Table 3 Damage cases of Example II

Damage Case II-1	A crack of 2 cm at left side of flange
Damage Case II-2	A crack of 4 cm at left side of flange
Damage Case II-3	Two cracks of 4 cm at left side and 2cm at right side of flange, respectively

welded zone of two flanges as shown in Fig. 11(a), and caused eventual severance of the member. Five PZT patches of 25×15×0.5 mm were attached to the outside surface of a flange as shown in Fig. 11(c). Damages were inflicted by cutting the flange at two locations sequentially, and three damage cases were constructed as described in Table 3. The impedance signatures were obtained for both lateral and thickness modes at the PZT patches in each damage case as shown in Figs. 12 and 13, respectively. As seen in Fig. 13, by taking an average with 128 times of data measurement, clearer signals were obtained compared with the case of Fig. 8.

Similarly to the former results, Fig. 13 depicting the impedances of thickness modes at the PZTs shows more significant variations in the impedance functions due to damages. At first, damage detection was carried out by comparing the resonant frequency shifts in the impedance functions at the thickness modes due to the damages. Fig. 14 presents the resonant frequency shifts at the PZTs after the damage cases. The results indicate that the crack locations may be effectively detected from the shifts of the resonant frequencies of the impedance functions obtained at the thickness modes of the PZT patches near the cracks. However, it shows that the crack detection becomes difficult as the crack occurs far from the PZT patches.

For the purpose of comparison, the RMS deviations of the impedance signatures for both lateral and thickness modes were also considered as the damage indicators. The results in Figs. 15 and 16 indicate that the RMS deviations can also give good information for damage detections. Particularly, the results for the thickness modes in Fig. 16 show that the accuracy of the crack detection is fairly similar to the cases using the shifts of the resonant frequency.

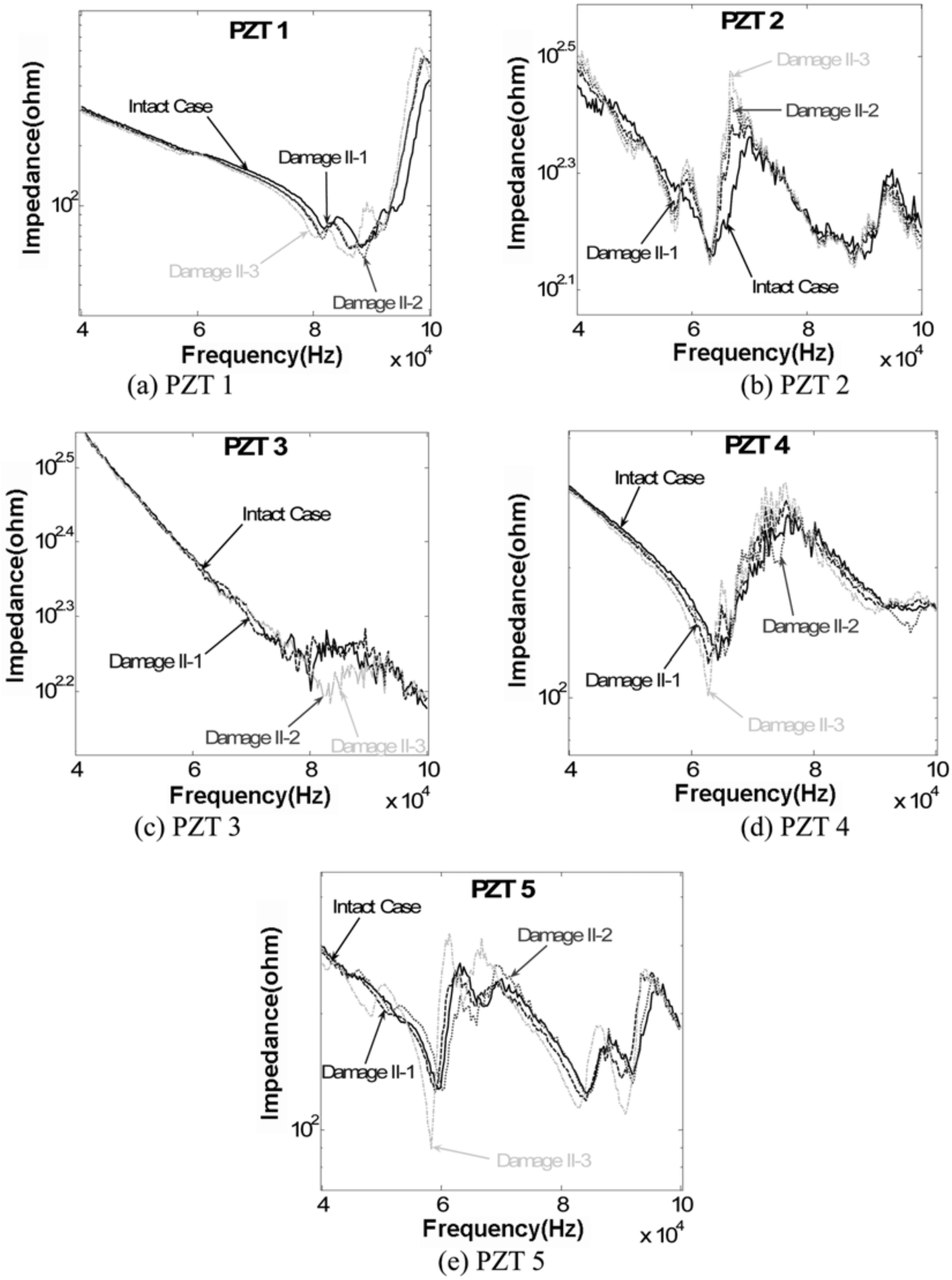

Fig. 12 Impedance signatures of lateral modes at PZT patches (in Magnitudes)

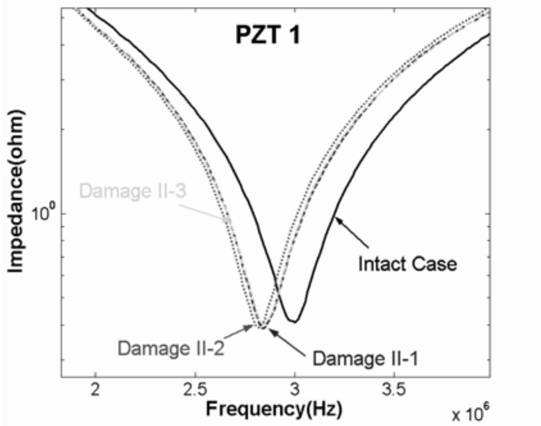

(a) PZT 1

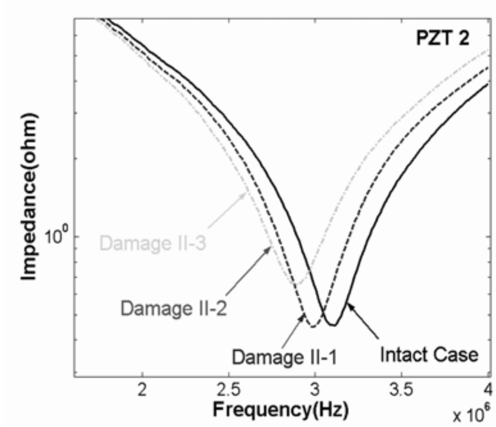

(b) PZT 2

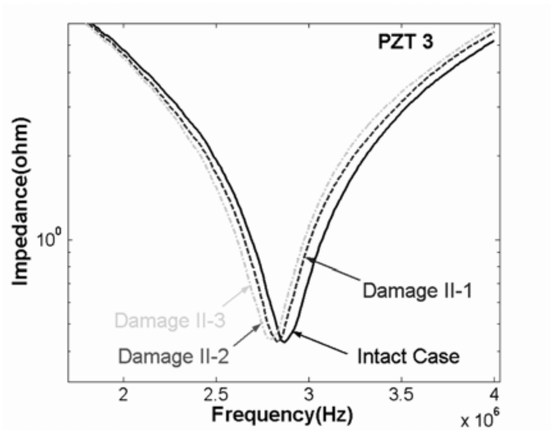

(c) PZT 3

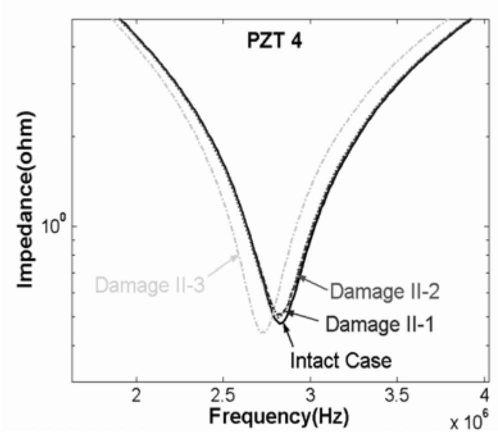

(d) PZT 4

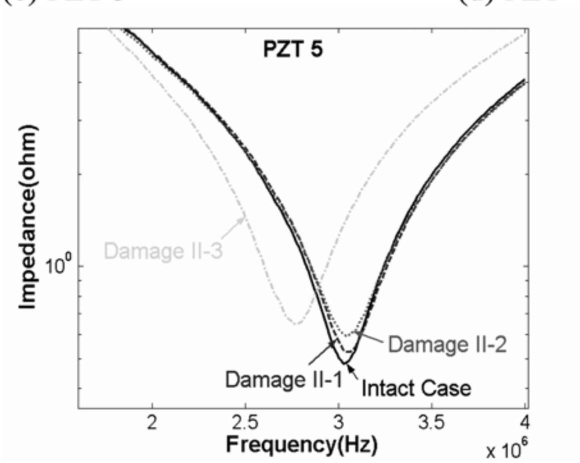

(e) PZT 5

Fig. 13 Impedance signatures of thickness modes at PZT patches (in Magnitudes)

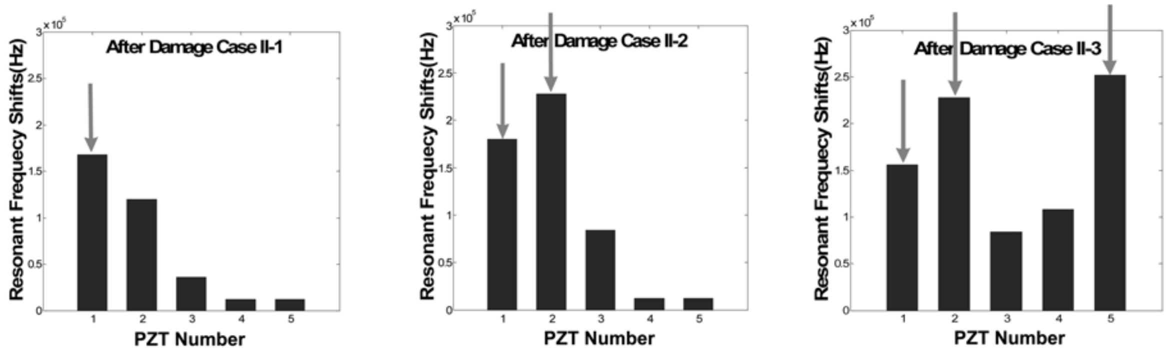

(a) Damage Case II-1 (b) Damage Case II-2 (c) Damage Case II-3

Fig. 14 Resonant frequency shifts of thickness mode-impedances after damages
(Note: Arrows indicate the locations of cracks.)

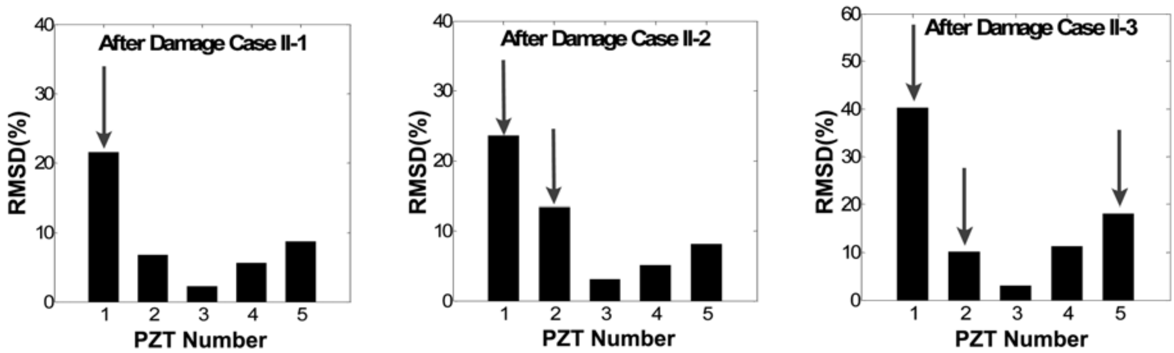

(a) Damage Case II-1 (b) Damage Case II-2 (c) Damage Case II-3

Fig. 15 RMS deviations of impedance functions of lateral modes at PZTs
(Note: Arrows indicate the locations of cracks.)

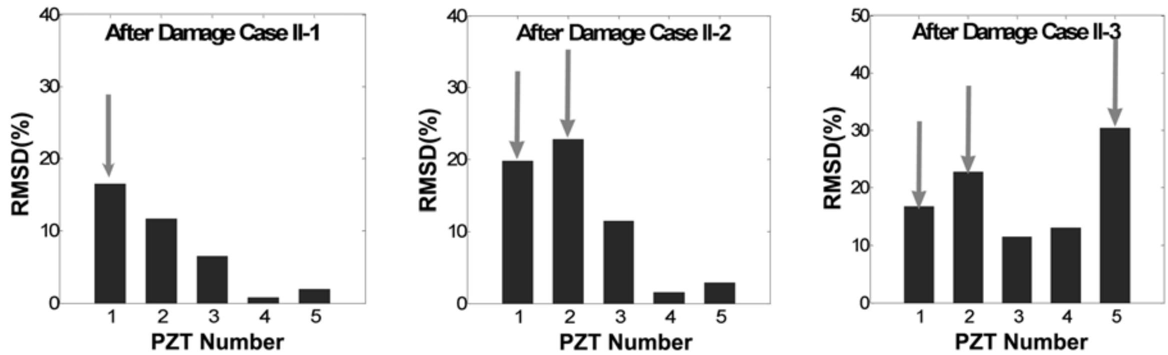

(a) Damage Case II-1 (b) Damage Case II-2 (c) Damage Case II-3

Fig. 16 RMS deviations of impedance functions of thickness modes at PZTs
(Note: Arrows indicate the locations of cracks.)

4. Conclusions

In this paper, the feasibility of PZT patches for detection of the localized damages in steel structures has been investigated through experiments on two kinds of steel structural members of laboratory size. The new concept to utilize thickness modes (frequency range > 1 MHz) of the PZT for impedance-based NDE techniques was proposed and investigated. This work is to supplement the capability for damage localizations of the conventional impedance-based structural health monitoring using lateral modes (frequency range > 20 kHz). The striking advantage of this thickness mode-impedance based damage detection method over the conventional lateral mode-impedance based method is that this technique shows more significant variations in resonant frequency shifts of the signals for identifying localities of small damages such as cracks.

In general, these PZT impedance-based NDE techniques are not requiring the knowledge of the modal parameters or the failure modes of the structure. And, while the global modes of structure at low frequencies are not affected by the localized damage, these impedance-based techniques which monitors the localized modes at high frequencies, can detect various local damages of the structures very successfully. Therefore, this technique facilitates an avenue for minimum labor involvement without having to be highly skilled. The PZT patch of even a small size (10×10×0.5 mm) has been ascertained to be very sensitive to incipient damages.

From the results of this study, following conclusions are obtained.

1. The impedance-based method using the thickness modes of the PZTs can detect the damages with more significant variations in the resonant frequency shifts of the signals than the lateral modes-based method for identifying the localities of small cracks of steel structures.
2. Both methods, however, can give good results for crack detection of steel structures by using the RMS deviations of the impedance functions of the PZTs.

Acknowledgements

The study was jointly supported by the Smart Infra-Structure Technology Center (SISTeC) at KAIST sponsored by the Korea Science and Engineering Foundation (KOSEF), and the Infra-Structure Assessment Research Center (ISARC) sponsored by Ministry of Construction and Transportation (MOCT), Korea. Their financial supports are greatly acknowledged.

References

Ayres, J. W., Lalande, F., Chaudhry, Z. and Rogers, C. A. (1998), “Qualitative impedance-based health monitoring of civil infrastructures”, *Smart Mater. Struct.* 7, 599-605.

Bhalla, S. and Soh, C. K. (2003), “Structural impedance based damage diagnosis by piezo-transducers”, *Earthquake Engineering Structural Dynamics*, **32**, 1897-1916.

Giurgiutiu, V. and Rogers, C. A. (1997), “Electro-mechanical (E/M) impedance method for structural health monitoring and nondestructive evaluation”, *International Workshop on Structural Health Monitoring*, 433-444, Stanford Univ., CA, September 18-20.

Kinsler, L. E. and Frey, A. R. (1962), *Fundamentals of Acoustics*, second edition, John Wiley & Sons, inc.

Park, G., Cudney, H. H. and Inman, D. J. (2000), “Impedance-based health monitoring of civil structural components”, *J. Infrastruct. Sys.*, **6**(4), December.

Park, G., Sohn, H., Farrar, C. R. and Inman, D. J. (2003), "Overview of piezoelectric impedance-based health monitoring and path forward", *The Shock and Vibration Digest*, **35**(6), 451-463, November.

Raju, V., Park, G. and Cudney, H. H. (1998), "Impedance-based health monitoring technique of composite reinforced structures", *Proc. of the 9th International Conf. on Adaptive Str. And Tech.*, 448-457, Cambridge, MA, October 14-16.

Sauerbrey, G. (1959), *Physics*, **155**(206).

Soh, C. K., Tseng, K. K.-H., Bhalla, S. and Gupta, A. (2000), "Performance of smart piezoceramic patches in health monitoring of a RC bridge", *Smart Mater. Struct.* **9**, 533-542.

Sun, F. P., Liang. C. and Rogers, C. A. (1994), "Experimental modal testing using piezoceramic patches as collocated sensors-actuators", *Proc. of the 1994 SEM Conf. & Exh.*, Baltimore, MI, June 6-8.

Tseng, K. K.-H., Soh, C. K., Gupta, A. and Bhalla, S. (2000), "Health monitoring of civil infrastructure using smart piezoceramic transducers", *Proc., 2nd Int. Conf. on Comp. Meth. for Smart Str. and Mat.*, 153-162.

Zagrai, A. N. and Giurgiutiu, V. (2001), "Electro-mechanical impedance method for crack detection in thin wall structures", *3rd Int. Workshop of Structural Health Monitoring*, Stanford Univ., CA, September 12-14.

"Piezoelectric Ceramics Properties and Applications" (2005), http://www.morganelectroceramics.com.

CC